Nanogold as a Specific Marker for Electron Cryotomography

Yongning He,[1] Grant J. Jensen,[1,2] and Pamela J. Bjorkman[1,2,*]

[1]Division of Biology, California Institute of Technology, 114-96, 1200 East California Blvd., Pasadena, CA 91125
[2]Howard Hughes Medical Institute, California Institute of Technology, 1200 East California Blvd., Pasadena, CA 91125

Abstract: While electron cryotomography (ECT) provides "molecular" resolution, three-dimensional images of unique biological specimens, sample crowdedness, and/or resolution limitations can make it difficult to identify specific macromolecular components. Here we used a 1.4 nm Nanogold® cluster specifically attached to the Fc fragment of IgG to monitor its interaction with the neonatal Fc receptor (FcRn), a membrane-bound receptor that transports IgG across cells in acidic intracellular vesicles. ECT was used to image complexes formed by Nanogold-labeled Fc bound to FcRn attached to the outer surface of synthetic liposomes. In the resulting three-dimensional reconstructions, 1.4 nm Nanogold particles were distributed predominantly along the interfaces where 2:1 FcRn-Fc complexes bridged adjacent lipid bilayers. These results demonstrate that the 1.4 nm Nanogold cluster is visible in tomograms of typically thick samples (∼250 nm) recorded with defocuses appropriate for large macromolecules and is thus an effective marker.

Key words: Nanogold, electron cryotomography, labeling, liposome, FcRn

INTRODUCTION

Electron microscopy (EM) has become a powerful technique to generate images of supramolecular structures (Lucic et al., 2005). Among various EM techniques, electron cryotomography (ECT) is a relatively new method that is suitable for three-dimensional (3D) structure determinations of large macromolecular complexes, cellular organelles, and intact cells *in situ* without involving the averaging procedures required by X-ray crystallography and single particle reconstructions. While in thin (<100 nm) and simple cryosamples, densities as small as individual proteins or even glycan strands can be recognized (Murphy & Jensen, 2005; Gan et al., 2008); in thicker, crowded, plastic-embedded, or complex samples, details are much harder to resolve and/or interpret (Henderson et al., 2007).

To help identify particular macromolecules, various types of gold particles have been used as markers (Hainfeld & Powell, 2000). The most commonly used gold particle in EM applications is colloidal gold, which can be made in different sizes and absorbed to antibodies for immuno-EM applications. Several properties of colloidal gold make it problematic as a specific label in high-resolution cryoEM studies. First, it absorbs nonspecifically to proteins, binding multiple molecules with variable stoichiometry. Second, it tends to aggregate to form large oligomeric gold-protein complexes, a particular problem for smaller (1–3 nm) colloidal gold particles. Finally, even small colloidal gold particles exhibit a fairly broad size distribution (Hainfeld & Powell, 2000).

More recently, homogeneous and well-behaved gold clusters such as Undecagold (Safer et al., 1986), Nanogold® (Hainfeld & Furuya, 1992), and monolayer protected clusters (Ackerson et al., 2006) that can be specifically and covalently bound to target macromolecules have been developed. When prepared with one linking group per gold particle, proteins can be labeled in a site-specific fashion with only one gold cluster per protein. Such cluster-labeled proteins are stable and not prone to aggregation, and are thus promising molecular labels.

Here we covalently attached 1.4 nm monomaleimido Nanogold to the Fc region of immunoglobulin G (IgG) to investigate the interaction between Fc and the neonatal Fc receptor (FcRn). FcRn is a receptor that transfers maternal IgG across epithelial cell barriers to mammalian offspring in order to passively immunize the newborn against environmental antigens and serves as a protection receptor to rescue IgG in the blood from a default degradative pathway (Roopenian & Akilesh, 2007). For both functions, FcRn binds to the Fc portion of IgG in acidic intracellular endosomes (pH 6.0–6.5) and releases IgG at the slightly basic (pH 7.4) pH of blood. Crystal structures of FcRn alone

(Burmeister et al., 1994*a*) and FcRn bound to Fc (Burmeister et al., 1994*b*; Martin et al., 2001) revealed the molecular details of the pH-dependent interaction between FcRn and IgG, but did not directly address how membrane-bound FcRn interacts with and transports IgG inside intracellular vesicles. Here we coupled FcRn to synthetic liposomes and incubated them with Nanogold-labeled Fc fragments to imitate the interaction between membrane-bound FcRn and IgG. We then used ECT to obtain 3D structural information concerning membrane-associated FcRn-Fc complexes. The direct visualization of 1.4 nm gold clusters by ECT suggests that it can be a useful single molecular marker to map the distribution of receptor-ligand complexes on membranes.

Materials and Methods

Liposome Preparation and FcRn Coupling

1,2-Dioleoyl-*sn*-glycero-3-phosphoethanolamine-N-[4-(p-maleimidophenyl) butyramide] (MBP-PE) (Avanti Polar Lipids, Inc.) lipids were dried and then hydrated with 20 mM Hepes pH 6.5, 0.15 M NaCl. A mini-extruder with a ~0.2 μm membrane was used to prepare liposomes. A soluble version of rat FcRn containing an introduced free cysteine (the K19C FcRn mutant) was purified from the supernatants of transfected CHO cells as described (Raghavan et al., 1995), incubated in 20 mM DTT, desalted on a Spin 6 desalting column, and then incubated overnight at room temperature with the MPB-PE liposomes in 20 mM Hepes pH 6.5, 150 mM NaCl. This reaction resulted in covalent coupling of the single free cysteine in the K19C FcRn mutant to the MPB-PE lipids through a thioether reaction (Martin & Papahadjopoulos, 1982). FcRn-coupled liposomes were concentrated using a Centraplus (100 kDa cutoff) and exchanged into 20 mM Hepes pH 6.0. The final coupling density for liposomes with diameters between 50 and 200 nm was estimated to be 70–1,000 receptors per liposome, calculated by dividing the liposome surface area (785,000–12,000,000 Å^2) by 11,000 Å^2, the approximate surface area covered by a glycosylated FcRn protein.

Preparation of Nanogold-Fc

We considered several types of metal clusters for labeling Fc (He et al., 2007). We were unable to observe FcRn binding by Fc proteins labeled with a 3 nm thiol-reactive monolayer-protected gold cluster (Ackerson et al., 2006) (kindly provided by C.J. Ackerson and R.D. Kornberg, Stanford University), and Fc proteins labeled with ultrasmall (~1 nm) or larger colloidal gold clusters formed aggregates that did not bind detectably to FcRn (data not shown). By contrast, Fc proteins labeled with 1.4 nm monomaleimido Nanogold retained pH-dependent binding to FcRn and showed no detectable aggregation as monitored by gel filtration chromatography (He et al., 2007).

Purified rat Fc (Martin & Bjorkman, 1999) was labeled with 1.4 nm monomaleimido Nanogold (Nanoprobes, Inc.) following the manufacturer's protocol. The resulting Nanogold-labeled Fc was separated from unlabeled Fc and free Nanogold by gel filtration chromatography, and then purified further by FcRn affinity chromatography (He et al., 2007). This procedure guaranteed that Nanogold-Fc preparations contained no detectable aggregates and that labeled Fc retained pH-dependent binding to FcRn. Nanogold/Fc ratios determined spectrophotometrically and estimated by SDS-PAGE were typically 0.8–1.1 (He et al., 2007), suggesting that most Fc molecules were singly labeled.

ECT Data Collection and Reconstruction

FcRn-coupled liposomes were incubated with unlabeled Fc fragment or Nanogold-labeled Fc under similar conditions. After 30 min at room temperature, 2 μL of each sample were mixed with 2 μL of 10 nm colloidal gold (as fiducial markers for alignment), loaded onto glow-discharged Lacey-carbon grids (Ted Pella, Inc.), and plunge frozen in liquid ethane at liquid nitrogen temperature. For two-dimensional (2D) imaging (see Fig. 2), cryoEM was performed on a FEI Tecnai 12 microscope operating at 120 kV at 2 μm defocus with a dose of ~20e/A^2 per image, and images were recorded on a 2X × 2K CCD at a magnification of 42,000×. For tomographic reconstructions (see Fig. 3), tilt series (−60° to 60°; 1.5° step size) were collected using a FEI Tecnai F30 microscope operating at 300 kV and controlled by a software package developed at University of California, San Francisco (Zheng et al., 2007). The defocus was set to 4.5–8.0 μm at 0°. Images were recorded with a 2K × 2K CCD at a magnification of 34,000× with a total dose of 80–100e$^-$/Å^2 for each tilt series. The IMOD software package (Kremer et al., 1996) was used for data processing and 3D reconstructions. A total of 23 independent tilt series were collected and reconstructed, with representative tomograms shown in Figure 3 and Supplementary Movie 1.

Results

FcRn is normally a type I membrane protein composed of a heavy chain with a single transmembrane spanning region and a noncovalently attached soluble light chain (β2-microglobulin) (Roopenian & Akilesh, 2007) (Fig. 1A). The ectodomain of a membrane protein can be attached to outer surface of a liposome through covalent or noncovalent binding so as to mimic the orientation of the membrane-bound version in a bilayer. For example, His-tagged protein ectodomains have been captured and oriented on nickel-NTA lipids (Celia et al., 1999). This method is not suitable for studies of the FcRn-Fc interaction, however, because the nickel/His-tag interaction is stable at basic, but not acidic pH, whereas FcRn binds to Fc only at acidic pH (Roopenian & Akilesh, 2007). As an alternate method to attach the
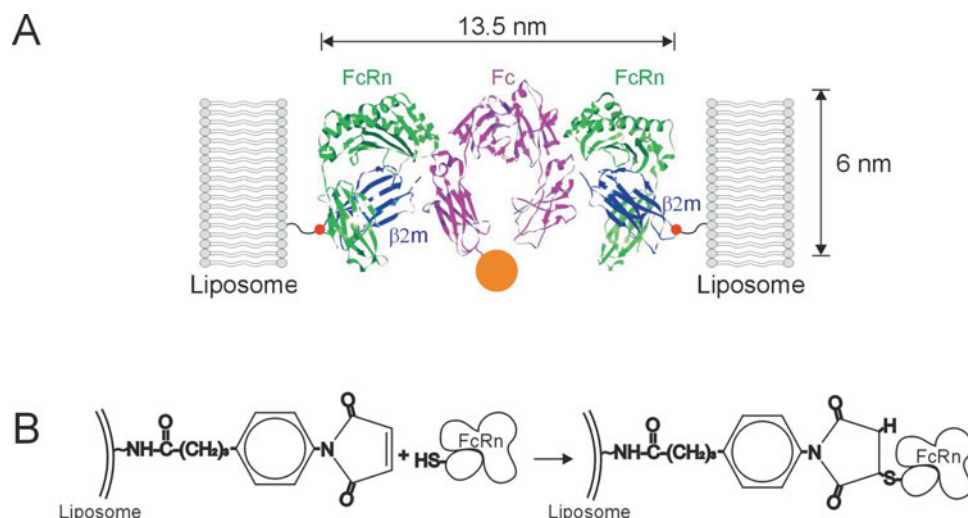
Figure 1. Preparation of FcRn-liposomes. **A:** Ribbon diagram of a 2:1 FcRn-Fc complex (pdb code 1I1A). A 1.4 nm Nanogold cluster (gold) is shown attached specifically to the reduced hinge region of the Fc. Residue 19 of the FcRn light chain (β2-microglobulin), which was mutated to cysteine in the K19C FcRn mutant, is highlighted as a red sphere with a linker attaching it to the liposome surface. **B:** Coupling of the FcRn ectodomain to liposomes. The K19C FcRn mutant was covalently coupled to the outer leaflet of liposomes through a thioether reaction between the introduced free cysteine in β2-microglobulin and the headgroup of MPB-PE.
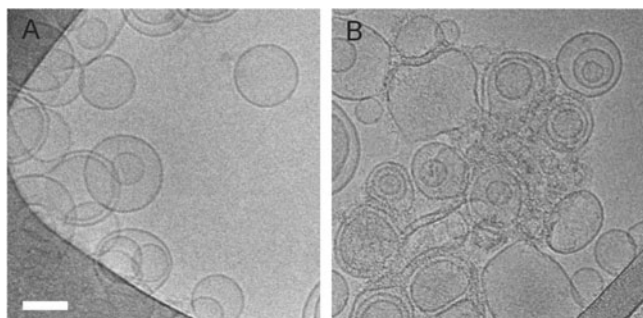

Figure 2. CryoEM images of FcRn-coupled liposomes. Scale bar = 100 nm. **A:** 2D projection in the absence of unlabeled Fc. **B:** 2D projection in the presence of unlabeled Fc.

soluble FcRn ectodomain to a liposome membrane, we used a previously described soluble rat FcRn mutant (K19C) in which the receptor light chain contained a free cysteine (Raghavan et al., 1995) and linked it covalently to MPB-PE lipids (Fig. 1B). The substitution in the K19C FcRn mutant is distant from the Fc binding site (Martin et al., 2001), and the K19C mutant functioned normally in pH-dependent binding of IgG when coupled covalently via the introduced cysteine to a biosensor surface (Raghavan et al., 1995), therefore coupling to lipids was not expected to disrupt FcRn-Fc recognition on a membrane surface.

FcRn-coupled liposomes were examined by cryoEM in the presence and absence of Fc at pH 6. In the absence of

Fc, most of the liposomes were isolated spherical structures with diameters ranging from 50 to 200 nm (Fig. 2A). The majority of the liposomes were unilamellar, but some contained one or two inner vesicles. Upon the addition of purified rat Fc, the liposomes showed increased aggregation with visible density between adjacent lipid bilayers (Fig. 2B). Many of the aggregated liposomes were flattened at the interface at which they interacted with an adjacent liposome. The inner vesicles of aggregated liposomes, which would not have access to FcRn or Fc, remained spherical. Given that FcRn can bind to both chains of a homodimeric Fc molecule to form a 2:1 FcRn/Fc complex (Huber et al., 1993; Martin & Bjorkman, 1999), these results suggested that the addition of Fc caused bridging between adjacent FcRn-coupled vesicles through the binding of FcRn molecules on separate vesicles to the same Fc dimer.

To further explore the bridging structure created by Fc addition to FcRn liposomes, we used ECT to generate 3D reconstructions of adhering liposomes. In the resulting tomograms, most of the interfaces between two adjacent lipid membranes showed continuous densities between bilayers (Fig. 3A). The typical distance between adjacent membranes in an interface was ~150 Å, consistent with the width of a 2:1 FcRn-Fc complex (Fig. 1A). However, the limited resolution of the tomograms did not permit conclusive identification of individual complexes. To gain more information about the interaction between Fc and FcRn-coupled liposomes, we repeated the ECT imaging using 1.4 nm Nanogold-labeled Fc. As previously described, mono-
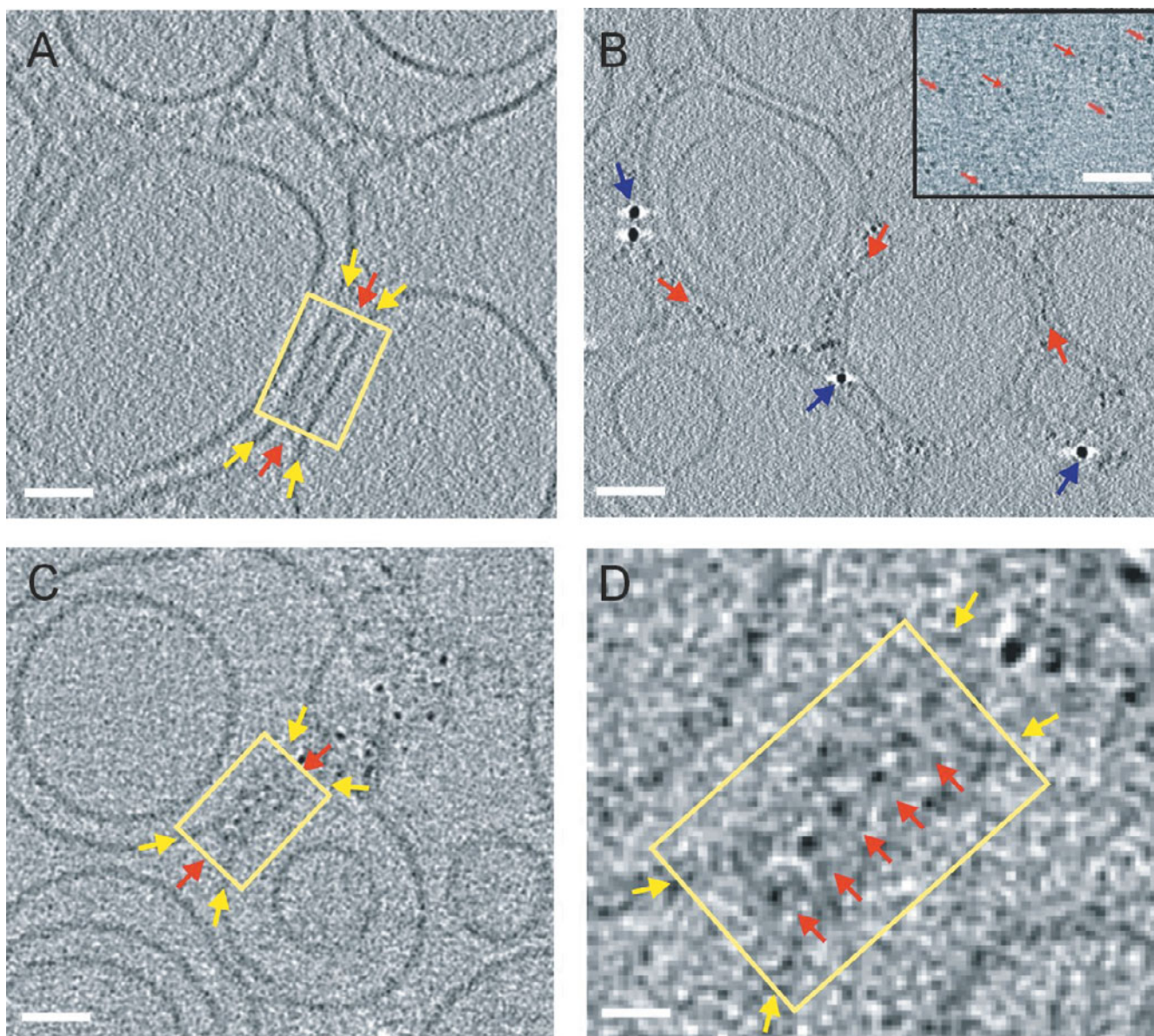
Figure 3. Tomographic slices (6.8 nm each) of FcRn-liposome plus Fc. Similar results were observed in 23 independent tomograms. **A:** Interface (yellow rectangle) formed between two adjacent liposomes bridged by unlabeled Fc showing continuous density (red arrows) between the adjacent membrane bilayers (yellow arrows). Scale bar = 45 nm. **B:** Overview of a field of FcRn-liposomes demonstrating that densities corresponding to 1.4 nm Nanogold-Fc (red arrows) are distributed exclusively at the interfaces between adjacent liposomes. Positions of 10 nm colloidal gold fiducial markers are indicated with blue arrows. Inset: 1.4 nm Nanogold-Fc in the absence of FcRn-liposomes (6.8 nm tomographic slice derived from a region of the grid over a hole). Nanogold clusters were identified as dark densities, each ∼2 nm in diameter (2–3 pixel, 0.68 nm/pixel), corresponding to the diameter of a single cluster plus the maleimido protecting groups. Scale bar = 60 nm. **C:** Interface (yellow rectangle) formed between two adjacent liposomes bridged by Nanogold-labeled Fc showing a row of gold clusters (red arrows) between the adjacent membrane bilayers (yellow arrows). Scale bar = 45 nm. **D:** Enlarged view of panel **C** demonstrating that the positions of individual 2:1 FcRn-Fc complexes can be identified by the gold cluster densities (red arrows). Scale bar = 10 nm.

maleimido Nanogold was covalently attached to the reduced sulfyhdral of the Fc hinge region, a site distant from the FcRn binding site (Fig. 1A), and the labeled Fc was purified by sizing and FcRn-affinity chromatography (He et al., 2007). The resulting Nanogold-labeled Fc functioned normally in FcRn binding and uptake into cells (He et al., 2007, 2008) and was therefore an appropriate reagent for these experiments.

When 1.4 nm Nanogold-labeled Fc was visualized in ice in the absence of FcRn-coupled liposomes, the gold clusters were randomly distributed (Fig. 3B; inset).

Supplementary Movie

When labeled Fc was added to the FcRn-coupled liposomes, the liposomes formed aggregates similar to those observed using unlabeled Fc, and the gold clusters were visualized clearly in tomograms (Fig. 3B–D; see Supplementary Movie at journals.cambridge.org/jid_MAM), mainly at the interfaces between adhering liposomes where density for FcRn-Fc complexes was observed (Fig. 3A).

Clusters appeared as dark densities, each ∼2 nm in diameter (2–3 pixel, 6.8 Å/pixel), corresponding to the diameter of a single Nanogold cluster plus the maleimido protecting groups. These dark densities were often in rows of 2 to 20 at the center of a liposome-liposome interface. The cluster densities were separated by at least ∼8 nm, consistent with the closest distances between adjacent FcRn-Fc complexes (Fig. 1A). These results suggested that cluster densities represented singly-labeled Fc molecules bridging between FcRn proteins coupled to adjacent liposomes.

The discovery of rows of 2:1 FcRn-Fc complexes bridging between adjacent membrane bilayers suggests that, as previously hypothesized (Burmeister et al., 1994b), FcRn can adopt a "lying-down" orientation with respect to the membrane (i.e., in which the long axis of the receptor is parallel to the bilayer) (Fig. 1A). Although this receptor orientation may occur on membranes under physiological conditions, electron tomographic studies of 1.4 nm Nanogold-labeled Fc inside transport vesicles of neonatal intestinal cells (He et al., 2008) suggest that 2:1 FcRn-Fc complexes are unlikely to bridge between the adjacent membranes of intracellular vesicles. This is because enhanced Nanogold-labeled Fc was observed inside intracellular compartments in which adjacent membranes were separated by ≥60 nm, a distance too large to span for bridging 2:1 FcRn-Fc complexes (Fig. 1A). It remains possible, however, that bridging 2:1 FcRn-Fc complexes could form at the cell surface between adjacent microvilli, where FcRn on the apical membrane of intestinal cells first encounter IgG in ingested milk (He et al., 2008).

Discussion

Small and defined gold clusters can be used to label proteins, peptides, or nucleic acids using specific chemistries to direct the labels to defined positions on the macromolecule of interest. These defined gold clusters are potentially useful for identifying the locations of molecules in EM applications (Safer et al., 1986; Hainfeld & Furuya, 1992; Ackerson

et al., 2006). Although too small to be routinely visualized in 2D projections or tomograms derived from plastic-embedded cellular samples (He et al., 2007), 1.4 nm Nanogold can be enlarged using traditional preembedding enhancement procedures in chemically-fixed samples (Weipoltshammer et al., 2000), and more recently, also in high pressure frozen/freeze substitution fixed samples (He et al., 2007; Morphew et al., 2008). We used the new enhancement methods to map individual 1.4 nm Nanogold-labeled Fc proteins within transport vesicles of high pressure frozen/freeze substitution fixed neonatal rodent intestinal cells (He et al., 2008).

Because enhancement procedures to enlarge Nanogold clusters are not possible for frozen hydrated samples, small gold clusters must be visualized without enlargement in ECT applications. Direct visualization has been achieved in frozen samples processed by single particle reconstruction methods, which involve averaging over a large number of particles (Boisset et al., 1992; Montesano-Roditis et al., 2001). In addition, 1.4 nm Nanogold has been visualized in 2D projections from frozen hydrated samples (Jeon & Shipley, 2000). What has not been clear is whether individual clusters could be identified in cryotomograms of unaveraged complexes, which are frequently embedded in thicker (hundreds of nm) ice, imaged at higher defocuses, and low-pass filtered to remove high-frequency noise.

Here we demonstrated that 1.4 nm Nanogold can be reliably located in tomograms obtained from frozen hydrated samples. Nanogold was covalently attached to a 60 kD protein (the Fc fragment of IgG), which then interacted with a receptor, FcRn (also ∼60 kD), that was attached to the membrane of a liposome. When unlabeled Fc was incubated with FcRn-liposomes, we observed density for rows of FcRn-Fc complexes that bridged between adjacent liposome bilayers, but individual FcRn-Fc complexes were not distinguishable. By contrast, in the presence of Nanogold-labeled Fc, the locations of individual FcRn-Fc complex could be determined from the cluster densities. The clusters were clearly visible in tomograms recorded from 4.5 to 8 μm defocus, imaging conditions that simultaneously allowed protein densities and both leaflets of the liposome bilayer to also be resolved. Nanogold therefore proved to be an effective molecular label, despite the ∼250 nm thick ice and even though the tomograms were low-pass filtered to the first zero of the contrast transfer function (in this case between $\frac{1}{3}$ to $\frac{1}{4}$ nm^{-1}). Nanogold labeling should thus also be applicable to many other systems, such as virus-receptor or cell-cell interactions, and provides a useful tool to identify single molecules under frozen hydrated conditions.

Acknowledgments

References

ACKERSON, C.J., JADZINSKY, P.D., JENSEN, G.J. & KORNBERG, R.D. (2006). Rigid, specific, and discrete gold nanoparticle/antibody conjugates. *J Am Chem Soc* **128**, 2635–2640.

BOISSET, N., GRASSUCCI, R., PENCZEK, P., DELAIN, E., POCHON, F., FRANK, J. & LAMY, J.N. (1992). Three-dimensional reconstruction of a complex of human alpha 2-macroglobulin with monomaleimido Nanogold (Au1.4nm) embedded in ice. *J Struct Biol* **109**, 39–45.

BURMEISTER, W.P., GASTINEL, L.N., SIMISTER, N.E., BLUM, M.L. & BJORKMAN, P.J. (1994a). Crystal structure at 2.2 Å resolution of the MHC-related neonatal Fc receptor. *Nature* **372**, 336–343.

BURMEISTER, W.P., HUBER, A.H. & BJORKMAN, P.J. (1994b). Crystal structure of the complex of rat neonatal Fc receptor with Fc. *Nature* **372**, 379–383.

CELIA, H., WILSON-KUBALEK, E., MILLIGAN, R.A. & TEYTON, L. (1999). Structure and function of a membrane-bound murine MHC class I molecule. *Proc Natl Acad Sci USA* **96**, 5634–5639.

GAN, L., CHEN, S. & JENSEN, G.J. (2008). Molecular organization of gram-negative peptidoglycan. *Proc Natl Acad Sci USA* **105**, 18953–18957.

HAINFELD, J.F. & FURUYA, F.R. (1992). A 1.4-nm gold cluster covalently attached to antibodies improves immunolabeling. *J Histochem Cytochem* **40**, 177–184.

HAINFELD, J.F. & POWELL, R.D. (2000). New frontiers in gold labeling. *J Histochem Cytochem* **48**, 471–480.

HE, W., KIVORK, C.K., MACHINANI, S., MORPHEW, M.K., GAIL, A.M., TESAR, D.B., TIANGCO, N.E., MCINTOSH, J.R. & BJORKMAN, P.J. (2007). A freeze substitution fixation-based gold enlarging technique for EM studies of endocytosed nanogold-labeled molecules. *J Struct Biol* **160**, 103–111.

HE, W., LADINSKY, M.S., HUEY-TUBMAN, K.E., JENSEN, G.J., MCINTOSH, J.R. & BJORKMAN, P.J. (2008). FcRn-mediated antibody transport across epithelial cells revealed by electron tomography. *Nature* **455**, 542–546.

HENDERSON, G.P., GAN, L. & JENSEN, G.J. (2007). 3-D ultrastructure of *O. tauri*: Electron cryotomography of an entire eukaryotic cell. *PLoS ONE* **2**, e749.

HUBER, A.H., KELLEY, R.F., GASTINEL, L.N. & BJORKMAN, P.J. (1993). Crystallization and stoichiometry of binding of a complex between a rat intestinal Fc receptor and Fc. *J Mol Biol* **230**, 1077–1083.

JEON, H. & SHIPLEY, G.G. (2000). Localization of the N-terminal domain of the low density lipoprotein receptor. *J Biol Chem* **275**, 30465–30470.

KREMER, J.R., MASTRONARDE, D.N. & MCINTOSH, J.R. (1996). Computer visualization of three-dimensional data using IMOD. *J Struct Biol* **116**, 71–76.

LUCIC, V., FORSTER, F. & BAUMEISTER, W. (2005). Structural studies by electron tomography: From cells to molecules. *Annu Rev Biochem* **74**, 833–865.

MARTIN, F.J. & PAPAHADJOPOULOS, D. (1982). Irreversible coupling of immunoglobulin fragments to preformed vesicles. An improved method for liposome targeting. *J Biol Chem* **257**, 286–288.

MARTIN, W.L. & BJORKMAN, P.J. (1999). Characterization of the 2:1 complex between the class I MHC-related Fc receptor and its Fc ligand in solution. *Biochem* **38**, 12639–12647.

MARTIN, W.L., WEST, A.P., GAN, L. & BJORKMAN, P.J. (2001). Crystal structure at 2.8 Å of an FcRn/heterodimeric Fc complex: Mechanism of pH dependent binding. *Mol Cell* **7**, 867–877.

MONTESANO-RODITIS, L., GLITZ, D.G., TRAUT, R.R. & STEWART, P.L. (2001). Cryo-electron microscopic localization of protein L7/L12 within the *Escherichia coli* 70 S ribosome by difference mapping and Nanogold labeling. *J Biol Chem* **276**, 14117–14123.

MORPHEW, M., HE, W., BJORKMAN, P.J. & MCINTOSH, J.R. (2008). Silver enhancement of nanogold particles during freeze substitution fixation for electron microscopy. *J Microsc* **230**, 263–267.

MURPHY, G.E. & JENSEN, G.J. (2005). Electron cryotomography of the *E. coli* pyruvate and 2-oxoglutarate dehydrogenase complexes. *Structure* **13**, 1765–1773.

RAGHAVAN, M., WANG, Y. & BJORKMAN, P.J. (1995). Effects of receptor dimerization on the interaction between the class I MHC related Fc receptor and immunoglobulin G. *Proc Natl Acad Sci USA* **92**, 11200–11204.

ROOPENIAN, D.C. & AKILESH, S. (2007). FcRn: The neonatal Fc receptor comes of age. *Nat Rev Immunol* **7**, 715–725.

SAFER, D., BOLINGER, L. & LEIGH, J.S., JR. (1986). Undecagold clusters for site-specific labeling of biological macromolecules: Simplified preparation and model applications. *J Inorg Biochem* **26**, 77–91.

WEIPOLTSHAMMER, K., SCHOFER, C., ALMEDER, M. & WACHTLER, F. (2000). Signal enhancement at the electron microscopic level using Nanogold and gold-based autometallography. *Histochem Cell Biol* **114**, 489–495.

ZHENG, S.Q., KESZTHELYI, B., BRANLUND, E., LYLE, J.M., BRAUNFELD, M.B., SEDAT, J.W. & AGARD, D.A. (2007). UCSF tomography: An integrated software suite for real-time electron microscopic tomographic data collection, alignment, and reconstruction. *J Struct Biol* **157**, 138–147.